

University of California  
Santa Barbara

# **Developing An Opto-Electronic Imaging System For Organoids**

A dissertation submitted in partial satisfaction  
of the requirements for the degree

Bachelors of Science  
in  
Physics

by

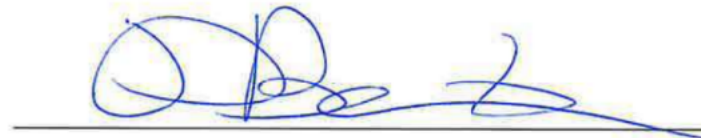
Samantha Herman

Committee in charge:

Professor Dirk Bouwmeester, Chair

December 2023

The Dissertation of Samantha Herman is approved.

A handwritten signature in blue ink, appearing to read "D. Bouwmeester", is placed above a horizontal line.

Professor Dirk Bouwmeester, Committee Chair

December 2023

Developing An  
Opto-Electronic Imaging System  
For Organoids

Copyright © 2023

by

Samantha Herman

**Abstract**

Developing An  
Opto-Electronic Imaging System  
For Organoids

by

Samantha Herman

Organoids are miniature organs grown from stem cells whose applications span pharmacology, neuroscience, and biophysics. Previous work studying organoids makes use of techniques involving calcium imaging for optical recordings or extracellular voltage stimulation and readout using Microelectrode Arrays (MEAs), but each of these methods introduces biases, obfuscating our understanding of the organoids being studied. Here I present the design, fabrication, and development of a transparent MEA and an opto-electronic imaging system designed to enable simultaneous voltage stimulation and calcium imaging. This architecture will allow both techniques for studying organoids to be used in tandem, permitting biases introduced by one technique to be exposed by the other technique, and vice versa. This work presents a proof-of-concept prototype which future work should build upon to incorporate an electrophysiology readout and increase electrode density in order to compete with commercially available MEAs.

## Acknowledgements

I would like to thank Dr. Dirk Bouwmeester for his support of me as a researcher in addition to supporting my visions for the future of this project. I would like to acknowledge Eve Bodnia's support, guidance, and mentorship throughout this project—especially with respect to supporting access to the nanofabrication facilities and initial characterization of fabrication recipes.

For constant assistance with the biology aspects of this project as well as 3D printing the majority of my fixture designs, I'd like to recognize Markus Merk. I'd like to thank Kellan Colburn for his assistance in troubleshooting numerous steps of my process (especially after I'd unintentionally inverted my mask designs), as well as for his help in dealing with the administrative hassle of purchasing various electronic components. Additionally, I'd like to acknowledge Hawkins Clay for teaching me how to wire bond, as well as for helping me troubleshoot issues with bonding to ITO and gold. For printing the high density production fixtures and enclosures I'd like to thank Brian Dincau. Finally, I'd like to recognize Majid Mohammad for his assistance in troubleshooting issues with wire bonding, deposition of contact pads, and generally for supporting me throughout this project.

The authors acknowledge the use of tools within the California NanoSystems Institute and the Nanofabrication Facility, supported by the University of California, Santa Barbara and the University of California, Office of the President.

# Contents

<b>Abstract</b>	<b>iv</b>
<b>Acknowledgements</b>	<b>v</b>
<b>1 Introduction</b>	<b>1</b>
1.1 Organoids . . . . .	1
1.1.1 Cardiomyocytes . . . . .	2
1.1.2 Neurons . . . . .	3
1.2 Microelectrode Arrays (MEAs) . . . . .	4
<b>2 Transparent MEA</b>	<b>8</b>
2.1 Nanofabrication Techniques . . . . .	8
2.1.1 Maskless Photolithography . . . . .	9
2.1.2 Electron Beam Physical Vapor Deposition . . . . .	10
2.1.3 Plasma-Enhanced Chemical Vapor Deposition . . . . .	11
2.1.4 Reactive Ion Etching . . . . .	12
2.1.5 Liftoff . . . . .	13
2.2 Process Recipes . . . . .	14
2.2.1 Transparent Electrodes . . . . .	15
2.2.2 Gold Bond Pads . . . . .	23
2.3 Electrical Resistance . . . . .	27
<b>3 Electronics Design</b>	<b>28</b>
3.1 Voltage Stimulation Platform . . . . .	29
3.1.1 Electromagnetic Compatibility . . . . .	30
3.1.2 Digital to Analog Conversion . . . . .	31
3.1.3 Serial Peripheral Interface . . . . .	32
3.1.4 Software . . . . .	34
3.1.5 Platform Assembly . . . . .	35
3.2 BNC Board . . . . .	37
3.2.1 Wire Bonding . . . . .	38

<b>4</b>	<b>Plating Cells</b>	<b>39</b>
4.1	Environmental Conditions . . . . .	39
4.2	Sterilization . . . . .	40
4.3	Cell Plating . . . . .	41
<b>5</b>	<b>Results</b>	<b>44</b>
5.1	System Operation . . . . .	45
<b>6</b>	<b>Conclusion</b>	<b>48</b>
6.1	Experiments . . . . .	48
6.2	Next Steps . . . . .	49
	<b>Bibliography</b>	<b>52</b>

# Chapter 1

## Introduction

At the heart of many fundamental and far-reaching questions in biology, neuroscience, pharmacology, and genetics is the study of the human body and the organs which comprise it. The development of an integrated transparent microelectrode array (MEA) is an important step in seeking to understand and potentially answer these questions, as it provides a platform upon which to electrically stimulate organoids while observing the results optically. Recordings made with these devices both literally and figuratively offer a window into the intricate world of organ development and function.

### 1.1 Organoids

Organs are complex masses of tissue made of billions of cells working in tandem to perform the processes that keep the body functioning. As the cells that make up these organs decay and die, they may be replaced by stem cells—cells that have the ability to differentiate into any other type of cell.

One use of stem cells is to create three dimensional cell cultures known as organoids.

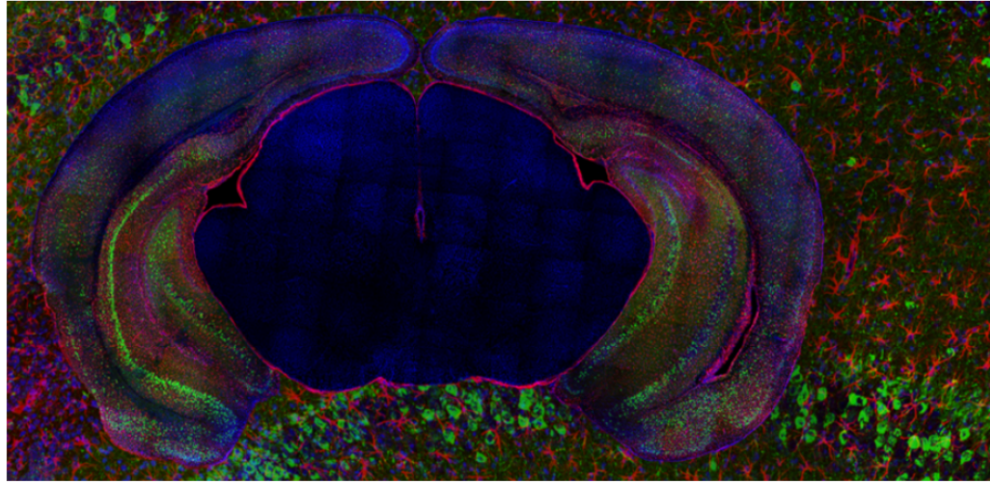


Figure 1.1: Cross section of brain organoid imaged under fluorescence microscopy.

These complex cell cultures are designed to replicate part or all of an organ's functionality based on the goals of the research being conducted. The miniature organs created are fully functional replicas of organs like the brain, kidney, lung, heart, intestine, liver, and stomach. They are measured to be as small as ten microns and as large as five millimeters [1].

Organoids can be dissected and studied to better understand how tissue develops, regenerates, and repairs itself. Additionally, they are useful for disease modeling, clinical drug studies, and creating tissue for personalized medical testing [2]. In particular, studying brain organoids and their corresponding constituents (neurons) delves into questions about the development of consciousness, quantum mechanics in the brain, and the possibility of growing biological computers.

### 1.1.1 Cardiomyocytes

A cardiomyocyte is the cell responsible for the contraction of the heart. With a centralized nucleus and a specific protein that distinguishes itself from other muscle

cells, the cardiomyocyte contracts rhythmically without rest. When cardiomyocytes are cultured on top of a microelectrode array (MEA), they attach to the surface and form a spontaneously beating layer of cells. Action potentials fired by a single cell propagate across the whole layer, causing all the other cells to fire and contract, which is detectable by the electrodes in the MEA. Providing external voltage stimulation through the electrodes offers a pathway to study the mechanisms by which artificial 'heartbeats' can be induced in the sheet of cardiomyocytes. Experiments of this nature conducted at various phases of cell development offer the potential to expand understanding of the development of the human heart.

### 1.1.2 Neurons

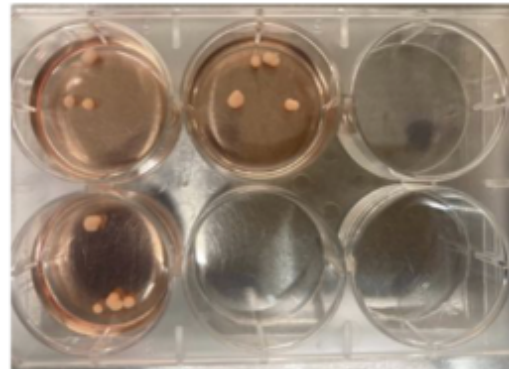


Figure 1.2: The organoids depicted are brain organoids consisting of neurons grown from human embryonic stem cells. They range in size from roughly 1 mm in diameter to 5 mm in diameter, and are stored in a temperature controlled environment.

Neurons are cells inside the brain and spinal cord responsible for ensuring that electrical and chemical signals are transported throughout the body. The dendrites and soma of a neuron form an electrically conducting pathway for electrical currents which through superposition induce a voltage potential at each point in space with respect to some reference point [3]. Because the electric field is the negative gradient

of the potential, measurements of the electric fields allow spatiotemporal resolution of signals propagating through neurons.

These currents generate both intracellular and extracellular voltages, the latter of which can be detected with MEAs. Because synaptic activity is often the largest source of extracellular current flow, MEAs are an excellent tool for measuring and studying local field potentials (extracellular currents generated from many different neurons simultaneously) and spikes (fast action potentials generated by a single neuron) [3]. When combined with calcium fluorescence markers like GCaMP, these spikes will cause photons to be emitted, making them an ideal candidate to be studied with optical imaging techniques using the transparent MEAs developed in this work [4].

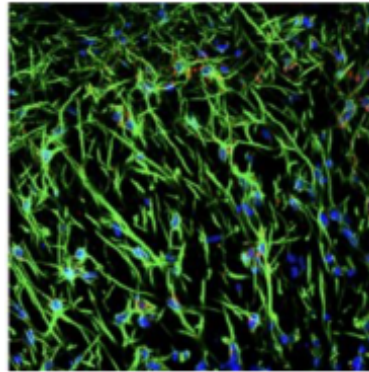


Figure 1.3: A two dimensional culture of neurons imaged under fluorescence microscopy. Displayed in green are the axonal segments of the neurons. The neurons' soma are highlighted in a blue color.

## 1.2 Microelectrode Arrays (MEAs)

In order to study organoids and their two dimensional cell culture counterparts, a device known as a microelectrode array or multielectrode array—the terms are used interchangeably—is used. These arrays come in a variety of different shapes and sizes, with the goal of providing an interface between the tissue being studied and the device

recording the data from the tissue.

Most MEAs consist of the same three components: electrodes, readout electronics, and stimulation electronics. The electrodes are made of a conductive, organic compatible metal such as gold or platinum and cover an area in the center of the MEA on which the tissue is grown or placed. The readout electronics contain components like low noise amplifiers and filtering stages, which are used to amplify potential differences in the electric field between each electrode and a much larger reference electrode. After being amplified, these signals can then be converted to digital signals and transferred to the recording device, typically a computer. At the same time, the stimulation electronics are used in conjunction with a signal generator to electrically stimulate the cells atop the electrodes by applying a controlled voltage to selected electrodes at a chosen frequency.

The majority of MEAs presented in the literature are devices whose method of representing the spatiotemporal activity of the tissue involves a simultaneous electrode readout. Each electrode has a known location on the array, and a recording taken from all electrodes simultaneously can give information about how signals travel across the tissue. For these studies, electrode density is an important hyperparameter that needs to be optimized to ensure maximum spatial resolution. As the spacing, or pitch, between electrodes decreases, it becomes possible to have multiple electrodes in contact with the same cell, permitting subcellular, cellular, and multicellular recordings and analysis to be performed.

However, traditional MEAs have a number of drawbacks—The electrophysiology recordings can be unreliable and biased due to tissue arrangement, weak electrical dipoles, and unfavorable cell morphology. Furthermore, sampling bias for active cells will often overestimate the prevalence of electrical spikes as compared to imaging

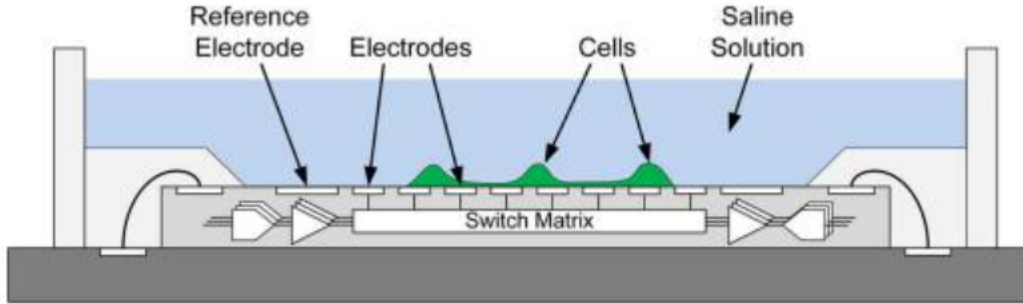


Figure 1.4: A block diagram of the 1024 channel CMOS microelectrode array with 26,400 electrodes built by Maxwell Electronics. The diagram displays the locations of cells grown atop an electrode sensing area, which are all encapsulated in a saline solution which contains the nutrients which keeps the cells alive. The Maxwell device additionally has a switch matrix which allows any arbitrary selection of a 1024 electrode subset of the 26,400 electrodes contained on the device. Reproduced from “A 1024-Channel CMOS Microelectrode Array” [5].

techniques, which are closer in line with estimates made by intracellular recordings [4].

The transparent MEAs presented in this work rely instead upon fluorescence microscopy and optical observation to represent the spatiotemporal activity of the tissue on the array. Increasing the electrode density necessitates the construction of complicated electronics to switch between electrode channels in addition to the electronics for signal filtration, amplification, and analog to digital conversion. Because neuronal signals have amplitudes ranging from 100 to 500 microvolts [5], to minimize the effects of path loss, amplifier noise, and switching noise, it is imperative that the amplification and conversion occur as close to the electrodes as possible. In traditional MEAs, these means that this circuitry is housed underneath the electrodes—but this configuration would defeat the advantages of transparent MEAs.

Though the ultimate goal for transparent MEAs is to combine electrical stimulation architecture with optical observation and the voltage readout paradigm described above, the devices presented in this work focus only on combining electrical stimula-

tion with optical recordings. This work seeks to sidestep the nuanced complexities of electrical engineering required to build a fully integrated voltage readout system while laying the foundation for it's development by creating a prototype that implements optical observation and electrical stimulation.

# Chapter 2

## Transparent MEA

Broadly, one can separate the transparent MEA developed in this work into three segments: The transparent substrate containing the microelectrodes and the nanofabrication techniques, masks, and recipes required to fabricate it; electronics design, device assembly, and the software architecture; and finally, the processes and protocols developed for sterilization and plating cells onto the device. This chapter focuses on nanofabrication tools, techniques, and recipes required for the fabrication of the transparent microelectrodes.

### 2.1 Nanofabrication Techniques

Nanofabrication techniques are essential for the development of transparent MEA, allowing for the precise control over electrode placement and size. In order to understand or replicate the top-level process workflow I developed for the fabrication of the transparent microelectrodes, it is necessary to first individually outline each of the major techniques used. This section presents an overview of the main procedures used to pattern electrodes into the substrate.

### 2.1.1 Maskless Photolithography

The goal of lithographic techniques in general is to transfer a pattern to the surface of the substrate undergoing lithography. In the case of this work, the surface in question happens to be a conductive and transparent layer of Indium Tin Oxide, and the pattern in question is that of the electrodes. Typical lithographic processes follow similar workflows: the surface is cleaned to remove particulate, then covered in a photosensitive polymer liquid known as photoresist. After thermally curing the photoresist, it is placed into the lithography tool where a beam of photons induces a series of chemical reactions which locally alters the pH of the surface. If the photoresist becomes more acidic, it is known as “positive” photoresist, whereas if it becomes less acidic it is known as “negative” photoresist. Post-lithography, placing the substrate in a bath in an alkali solution known as “developer” strips either the exposed (positive) photoresist or the unexposed (negative) photoresist. The leftover photoresist forms a sacrificial layer that protects the layer beneath it for subsequent processes [6].

In traditional photolithography, the photolithography tool uses a photomask to physically impedes the path of the photons on their way from the source to the substrate. Though photomasks are excellent for high throughput, high volume manufacturing of sub-micron features, they must be purchased or manufactured separately and have potentially long lead times. Because the smallest feature of my prototypes (the electrodes themselves) is 10 microns, using a maskless photolithography tool has no drawbacks during the prototyping stage of this work.

In maskless lithography, the pattern is exposed directly onto the surface of the substrate using a “dynamic photomask” known as a spatial light modulator (SLM). Designs uploaded to the tool are converted into a series of rectangular strips and are patterned into the substrate surface one strip at a time by moving the photon

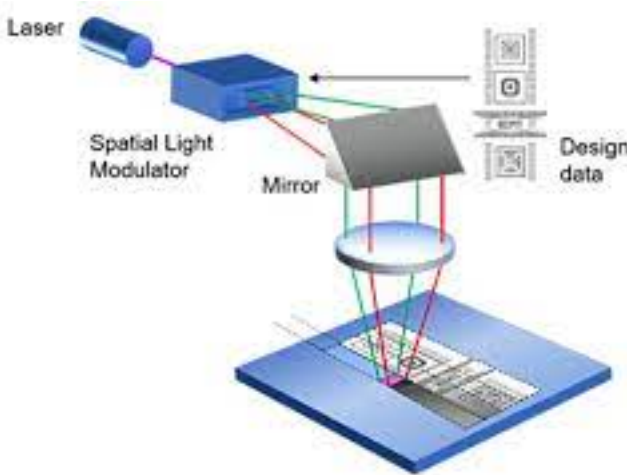


Figure 2.1: A Spatial Light Modulator (SLM)—essentially a dynamic mask—is used to project the design directly onto the wafer surface. The full image may consist of many individual images in stripe form. Reproduced from [7]

beam across the surface, instead of exposing the entire surface simultaneously as in standard techniques. So long as features are larger than a micron, this technique offers rapid prototyping for device R&D [7].

### 2.1.2 Electron Beam Physical Vapor Deposition

Electron beam Physical Vapor Deposition (PVD) is a deposition technique that uses a high energy beam of electrons to deposit thin films of a material onto a substrate. This technique is used to deposit a thin film of Indium Tin Oxide (ITO) onto the transparent substrate. ITO has a high melting point ( $>1500\text{ }^{\circ}\text{C}$ ), making it an excellent candidate for electron beam PVD due to the technique's propensity for the vaporization of high melting point materials with a relatively low deposition time.

In electron beam evaporation, a tungsten filament is heated up through the application of a voltage. This causes the thermionic emission of electrons at a rate given by the Boltzmann distribution. When the emitted electrons are accelerated, they

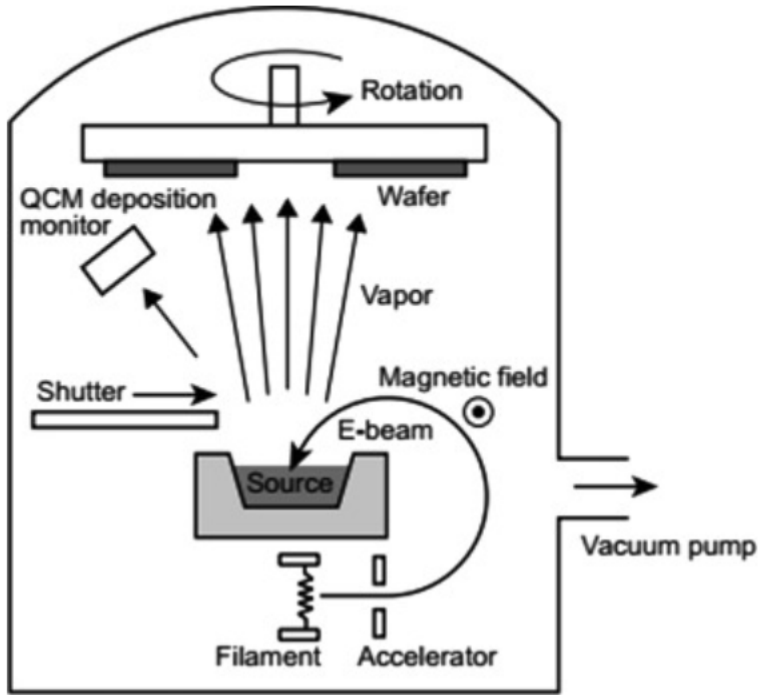


Figure 2.2: A schematic representation of electron beam physical vapor deposition. A beam of electrons emitted from the filament vaporize the source material through kinetic energy transfer. Reproduced from [6]

transfer enough kinetic energy upon impact to evaporate the source material. When the vapor reaches the substrate, it returns to a solid state of matter, uniformly coating the surface. To prevent the filament from being melted by the vapors, it is located out of sight of the evaporant, and an electromagnet is used to bend the beam to make contact with the source material [6].

### 2.1.3 Plasma-Enhanced Chemical Vapor Deposition

Chemical Vapor Deposition (CVD) processes deposit thin films of material through chemical reactions carried out in a vacuum chamber. The chemical reaction takes the material from a gaseous state (sometimes diluted by a carrier gas) to a solid state on the substrate. This process was used to deposit a thin film of silicon dioxide

atop the electrodes as insulation from electrical shorts. Silicon dioxide is deposited through the chemical reaction between silane and nitrous oxide.

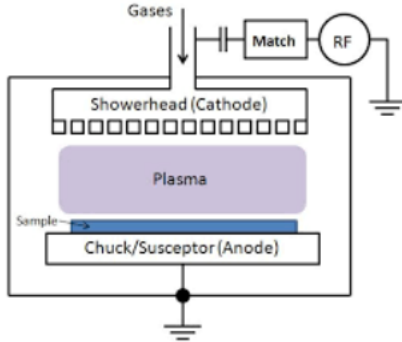


Figure 2.3: The RF potential across the cathode and anode of the chamber to generate a plasma, permitting the reaction to proceed at lower temperatures than possible through thermal CVD techniques. Reproduced from LNF PECVD wiki.

Plasma-enhanced CVD processes use molecule ionization to allow the chemical reactions to take place at a lower temperature. Because the mass of an electron is much lower than the mass of the atoms or molecules in the reaction and in a partially ionized plasma these ionized electrons have inefficient interactions with the neutral atoms, the electrons can be maintained at high equivalent temperatures. An RF power source is used to ignite the plasma through an RF potential difference across the cathode and anode of the chamber [6].

#### 2.1.4 Reactive Ion Etching

In general, the goal of etching is to transfer a pattern to a layer of material on top of a substrate. A sacrificial layer placed above the layer to be etched (usually photoresist) which is resistant to the etchant protects areas where etching is undesirable. In this way, material can be selectively removed, creating the desired pattern. In the case of the transparent MEA, Reactive Ion Etching (RIE) is used after maskless photolithography to remove excess ITO from the substrate to create the pattern

for the electrodes and Inductively Coupled Plasma (ICP) etching is used to open the electrodes underneath the insulating silicon dioxide layer.

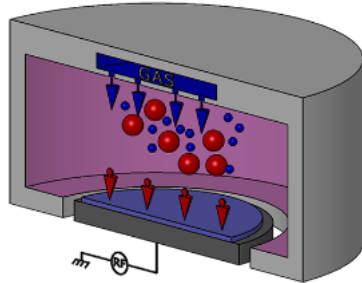


Figure 2.4: An RF potential ignites a plasma which through chemical reactions and ion bombardment etches the wafer on the anode (shown in blue). Choice of reactants, electric field strength, temperature, and gas pressure all affect the etch rate. Reproduced from [8].

Because of the precise control over etch rates through gas pressure, temperature, and electric field distribution, dry etching techniques like RIE are preferred in modern high volume processes [6]. In a typical RIE process, plasma is ignited by applying RF power to the powered electrode (the cathode) while the other electrode (the anode) is grounded. The electric field ionizes the gas molecules, creating the plasma. Once the plasma is established, a DC bias forms between the anode and cathode, extracting and accelerating ions from the plasma towards the surface of the cathode, and consequently, the wafer. A combination of chemical reactions and ion bombardment ultimately etches the material [8].

### 2.1.5 Liftoff

Liftoff is a technique used to create patterns by using an inversely patterned sacrificial layer, which is usually photoresist. In direct contrast to subtractive techniques like etching, liftoff is most useful when the substrate is fragile and would otherwise be damaged by etching or other subtractive techniques. For transparent

MEAs, it is used to pattern a thin film of gold onto the bond pads to improve the process of wire bonding to the MEA.

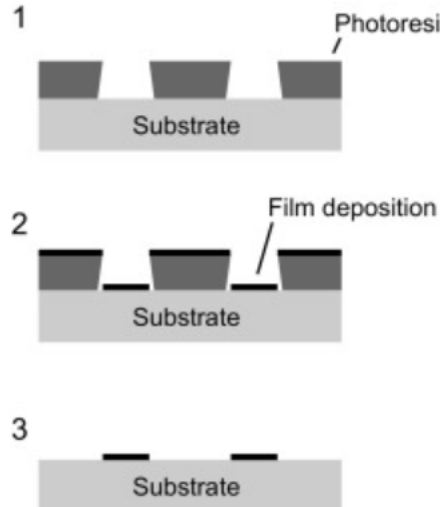


Figure 2.5: Visualization of the liftoff process. First, a sacrificial layer of photoresist is placed on the substrate. Then, a thin film of the target material is deposited. Finally, through sonication in a solvent, the photoresist (and any material atop the photoresist) is removed, leaving behind the desired pattern. Reproduced from [6]

A typical liftoff process flow is as follows: The inverse sacrificial layer of photoresist is deposited. Then, a thin film of the desired material is deposited. It is important that the film of material deposited is thinner than the sacrificial layer—otherwise, the solvent will be unable to attack the photoresist. Finally, the photoresist is removed, leaving behind the desired pattern. This process is usually done through sonication in a bath of a solvent like acetone [6].

## 2.2 Process Recipes

This section presents a detailed outline of the steps required in order to fabricate transparent MEAs. Many of these recipes were developed by the staff of the UCSB

nanofabrication facility for the individual tools in the facility, and may need to be tweaked slightly in order to be replicated on tools in other facilities. Section 2.2.1 discusses the recipes and procedures required to fabricate the transparent electrodes. Devices fabricated with this procedure are used in the voltage stimulation platform presented in Section 3.1. Section 2.2.2 discusses the recipes and procedures required to add gold contact pads to the transparent electrodes discussed in section 2.2.1. These contact pads enable gold to gold wire bonding, which is the mechanism for electrical connection to the BNC breakout board system presented in section 3.2.

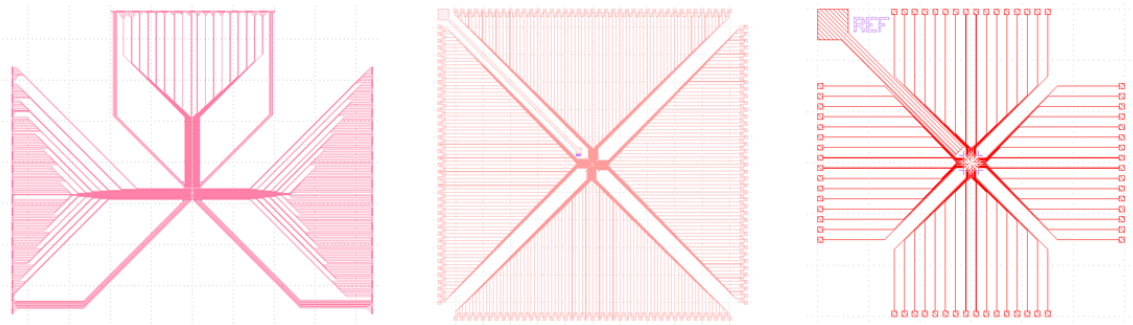


Figure 2.6: Presented is the Indium Tin Oxide (ITO) layer mask for three of my prototype electrode designs. They are presented from left to right in order of chronological development. All three designs contain all of their electrodes in a 2 mm x 2mm square sensing area in the center of the electrode array. The design on the left has 400 electrodes. To make manual wire bonding simpler, the bond pads on the edges were expanded in the middle design, resulting in a reduction to 324 electrodes. As shown on the right, the design was reduced to 64 electrodes to be compatible with the Intan RHD2164 Electrophysiology Interface Chip [9].

## 2.2.1 Transparent Electrodes

The substrate used for the transparent electrodes is a 4 inch wafer of high quality fused silica. For the system in section 3.1, the transparent MEA contains 64 electrodes and fills a 3 cm x 3 cm footprint. A four inch wafer provides enough space to comfortably fit four devices. For the system in section 3.2, the transparent MEA

contains 324 electrodes and fills a 5.65 cm x 5.65 cm footprint. A four inch wafer provides enough space to fit one device, with buffer on the edges. The steps for the process are as follows:

1. Standard clean of the blank fused silica substrate wafer. This process involves sonication for three minutes in a bath of acetone, followed by three minutes in a bath of isopropyl alcohol, followed by three minutes in a bath of deionized water in a variable power Crest-ultrasonic unit.
2. A custom Temescal Electron-Beam Evaporation System referred to internally by the UCSB nanofabrication facility as “E-beam two” uses Electron-beam Physical Vapor Deposition to deposit 75 nm of Indium Tin Oxide (ITO) onto the fused silica substrate, which is heated to 200°C. Because the temperature sensor

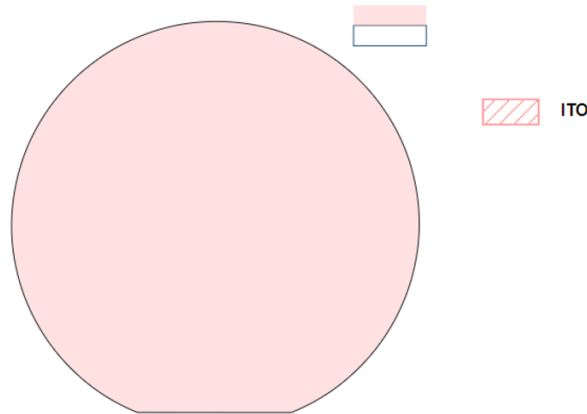


Figure 2.7: The circular figure represents a bird's eye view of the wafer, while the rectangular figure represents a cross section of the wafer. Indicated in red is Indium Tin Oxide (ITO). After the deposition step, a 75 nm thin film of ITO is on top of the fused silica substrate.

in the unit reads the chamber temperature, not the substrate temperature, an additional thermocouple on the unit reads the temperature of the wafer sample holder. To run the process, the chamber heat is put to a setpoint of 500°C, and

the process is started when the sample holder thermocouple reads 200°C. ITO is deposited at a rate of 0.5 Angstroms/sec.

3. After depositing ITO, a Headway PWM32 series photoresist spinner is used to uniformly apply HMDS adhesion promoter to the surface of the wafer. This entails using a pipette to drop the solution onto the wafer, attempting to avoid bubbles in the liquid. It should be spun at 3000 rpm until the liquid takes on a rainbow characteristic/color. Then, SPR 955 CM-0.9 positive photoresist should be dropped on top of the wafer using a pipette, once again attempting to avoid bubbles in the liquid. It should be spun at 3000 rpm for thirty seconds. This is followed by baking the wafer for sixty seconds at 90°C.

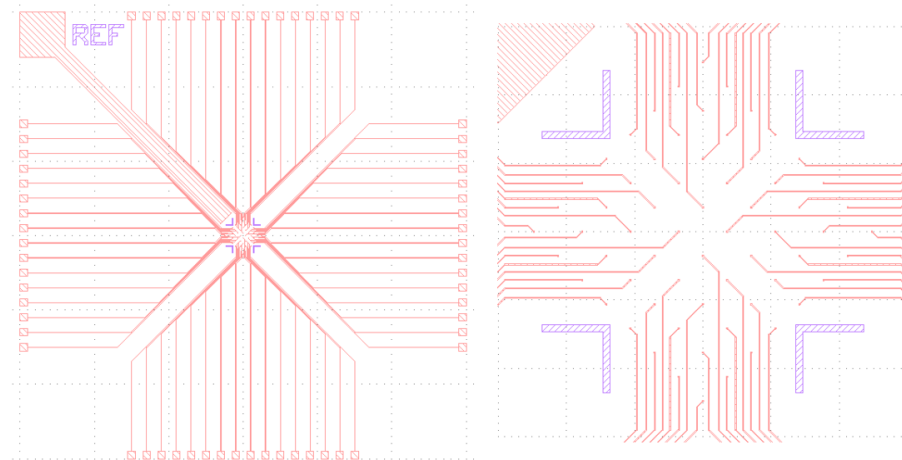


Figure 2.8: In step four of the process, the mask on the left is converted into rectangular strips for exposure by the Heidelberg MLA150 Maskless Aligner. Because the process uses positive photoresist, exposure followed by development will remove photoresist in the areas indicated in red. For this reason, the mask must be inverted. The image on the right is a close up of the electrode sensing area of the mask presented on the left.

4. After the photoresist has been applied and cured, it should be placed into the Heidelberg MLA150 Maskless Aligner. Once the wafer has been aligned with a rotation of 15 mRad or less, the wafer can be exposed with the electrode mask

displayed in figure 2.8. Because the photoresist is positive, the mask I designed needs to be inverted on this tool. The following parameters are used: dose ( $\text{mJ/cm}^2$ ) is 260, defocus is -7, laser is 405 nm, and the power is 100%. After exposure, the wafer is baked at 110°C for sixty seconds. Finally, it is developed in AZ MIF 300 for 90 seconds by vigorously shaking the wafer while holding it submerged with tweezers. The same process is repeated in deionized water for sixty seconds after development to clean it.

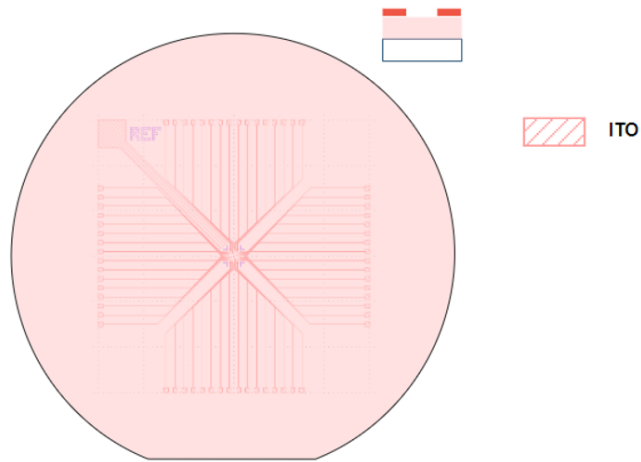


Figure 2.9: After performing photolithography and developing the photoresist on the surface of the substrate, the photoresist that remains (dark red) is patterned in the shape of the electrodes. It forms a sacrificial layer that will protect the ITO beneath it during the etching step, resulting in transference of the electrode pattern to the film of ITO.

5. Using a Materials Research Corporation RIE-51 parallel plate 13.56 MHz system, the wafer is etched to remove the excess ITO, creating transparent electrodes atop the transparent substrate. The system controls O<sub>2</sub>, CH<sub>4</sub>, H<sub>2</sub>, and Argon gas lines, which are used during etching to create an O<sub>2</sub> cleaning step and an MHA (CH<sub>4</sub>/H<sub>2</sub>/Ar) etching step. Prior to etching, the system is run for 30 minutes at a bias voltage of 500 V, a pressure of 125 mT, and 20 sccm of O<sub>2</sub>. Then, the system is seasoned by running for 20 minutes at a bias voltage

of 500 V, a pressure of 75 mT, and a 4/20/10 sccm mixture of CH<sub>4</sub>/H<sub>2</sub>/Ar.

After inserting the wafer, the first etching step of 4/20/10 sccm MHA is run at 75 mT and 350 V for five minutes. Then, a cleaning step of 20 sccm O<sub>2</sub> is run at 125 mT and 170 V for one minute. This is followed by a second etching step of 4/20/10 sccm MHA at 75 mT and 350 V for five minutes. Finally, there is a 20 sccm O<sub>2</sub> cleaning step at 125 mT and 170 V for five minutes.

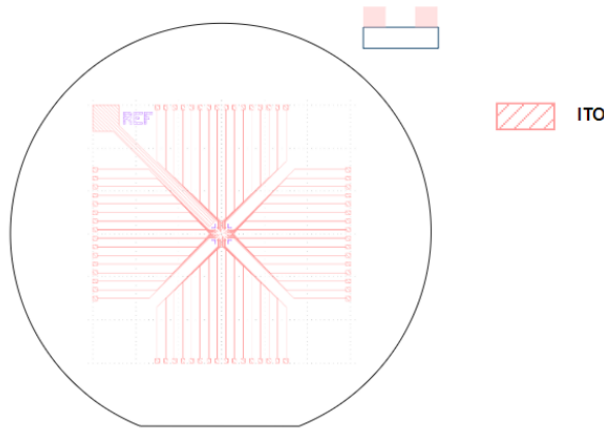


Figure 2.10: After etching, the ITO underneath the protective photoresist mask remains, while the rest of the ITO has been removed. The electrode pattern has been transferred to the sheet of ITO. Indicated in white is the fused silica substrate.

6. To clean the wafer before the next step and remove any debris, the substrate is subjected to a standard sonication clean consisting of 3 minutes of acetone, 3 minutes of isopropyl alcohol, and 3 minutes of deionized water, as before. Then, using the YES ecoclean plasma ash, a 3kW 180°C clean is performed for ten minutes. This strips any residual photoresist from the surface and prepares the surface for new material deposition.
7. To insulate the wires and prevent electrical shorts, a Plasma-Therm Vision 310 Advanced Vacuum PECVD system is used to deposit 100 nm of silicon dioxide using the standard SiO<sub>2</sub> recipe, which relies on a chemical reaction

between silane and nitrous oxide. Before placing the wafer into the chamber, it

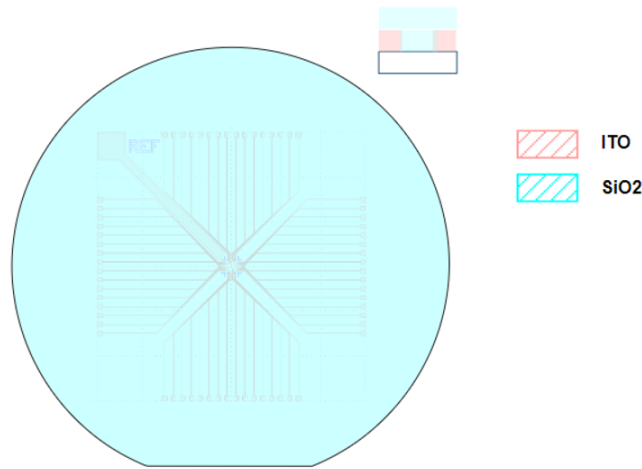


Figure 2.11: After the deposition of 100 nm of Silicon Dioxide (light blue), the electrodes patterned from ITO and the fused silica substrate are completely covered. This layer will prevent electrical shorts.

is seasoned for ten minutes with the standard (preprogrammed into the tool) recipe for SiO<sub>2</sub>. Then, the standard recipe is run for ten minutes of deposition.

8. Step 3 is repeated identically to spin photoresist onto the surface of the wafer.

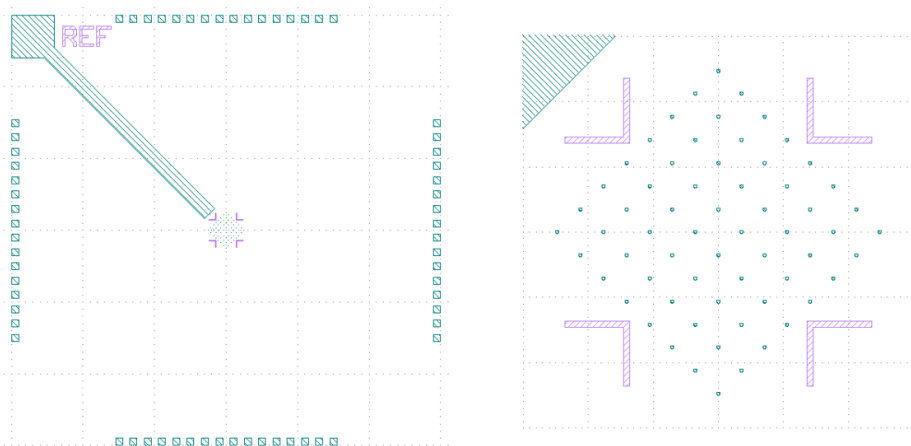


Figure 2.12: In step nine of the process, the mask on the left is converted into rectangular strips for exposure by the Heidelberg MLA150 Maskless Aligner. Because the process uses positive photoresist, exposure followed by development will remove photoresist in the areas indicated in dark green. For this reason, the mask must NOT be inverted as this is the pattern to be etched. The image on the right is a close up of the electrode sensing area of the mask presented on the left.

9. Then, step 4 is repeated with the same parameters previously mentioned. The only difference is that a different programmable photomask, presented in figure 2.12 is used. The photomask I designed for this step is intended to be used in the subsequent etching step to open holes above the electrodes and bond pads. Thus, because the photoresist used is positive, and exposing positive photoresist causes it to be removed during development, the design should NOT be inverted. After lithography, the same development step should follow.

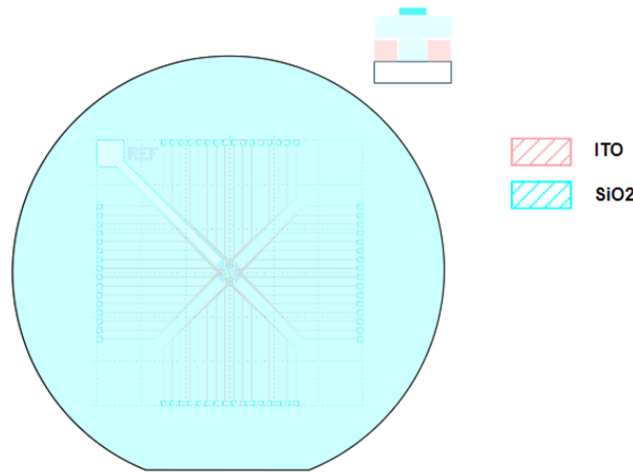


Figure 2.13: After exposing and developing the photoresist (bright blue) applied in step 8, the photoresist forms a protective coating for the etching step to follow. Indicated in slightly lighter blue are the bond pads, electrodes, and reference electrode, demonstrating that the photoresist covers the entire wafer with the exception of these areas.

10. Using a Panasonic Factory Solutions ICP etch tool, the SiO<sub>2</sub> layer of the wafer is opened to reveal electrodes and bond pads underneath. First, a cleaning wafer is placed into the robotic cassette, allowing a seasoning recipe of O<sub>2</sub> for ten minutes followed immediately by one minute of CF<sub>4</sub>. The transparent substrate is secured to a carrier wafer using a drop of santavac glue, and then placed into the chamber. Five minutes of the tool's silicon nitride etch is sufficient to etch through the 100 nm of silicon dioxide, using a gaseous mixture of CHF<sub>3</sub> and

O2. The substrate is removed from the carrier wafer through the application of copious quantities of acetone. In order to avoid shattering the wafer when removing it from the carrier wafer, razor blades can be used to slightly lift the edge of the wafer off the carrier. This permits more direct application of acetone to the underside of the substrate. Under no circumstances should this technique be used to lift the substrate from the carrier wafer, as this will cause it to fracture. It should instead be slid off the carrier wafer, adding acetone as needed to dissolve the glue.

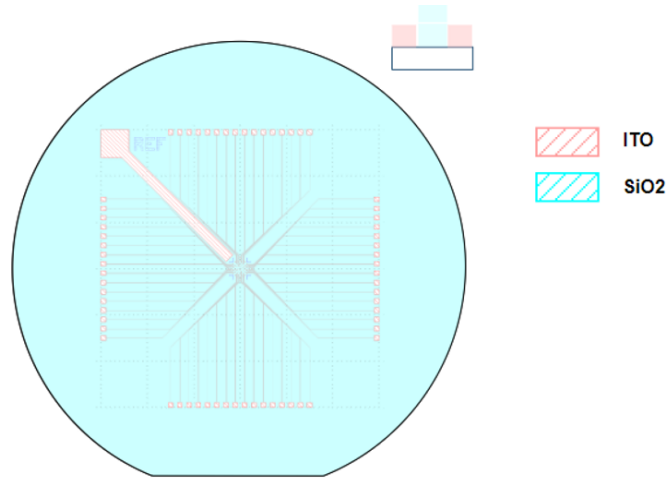


Figure 2.14: The electrodes and bond pads are opened after silicon dioxide etching. The blue layer atop the surface of the wafer indicates that all of the wires connecting the electrodes are covered in insulating silicon dioxide. The exposed red indicates that the ITO electrodes are accessible.

11. Once again, the wafer needs to be cleaned using the method outlined in step 6. This should remove any residual santavac glue, debris from etching, and residual photoresist. At this point, if it is desired to add a thin film of gold to the bond pads, continue to section 2.2.2. Otherwise, the wafer is ready to be diced. To protect the surface from scratches during the dicing process, it is recommended that a layer of photoresist be applied to the surface and cured. After dicing,

this photoresist will need to be cleaned off using the method outlined in step 6.

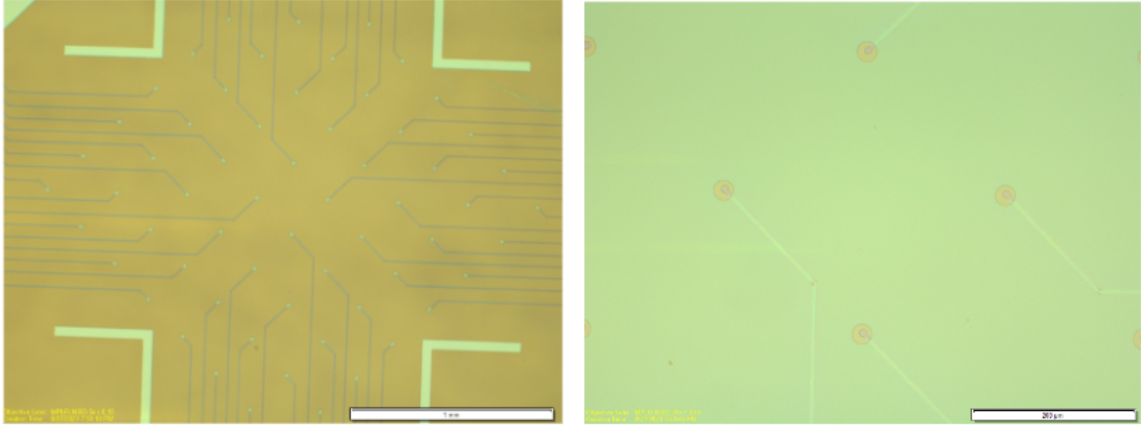


Figure 2.15: On the left is an image of the sensing area, where the 64 electrodes are located. The scale bar is 1 mm long. The sensing area covers a 2 mm x 2 mm area. On the right is a close up of four electrodes. The scale bar is 200 microns long. The openings in the silicon dioxide which expose the electrodes are shown in orange.

## 2.2.2 Gold Bond Pads

The recipe outlined in this section requires that the device outlined by the recipe in section 2.2.1 be completed through step 10. After the cleaning portion of step 11 is completed, in order to plate gold onto the bond pads, a liftoff process is necessary. The deposition of 100 nm of gold onto the bond pads allows gold to gold contact wire bonding to proceed smoothly, which is required for assembling the device outlined in section [?].

1. A Headway PWM32 series photoresist spinner is used to uniformly apply HMDS adhesion promoter to the surface of the wafer—silicon dioxide insulation atop a layer of patterned ITO electrodes. This entails using a pipette to drop the solution onto the wafer, attempting to avoid bubbles in the liquid. It should be spun at 3000 rpm until the liquid takes on a rainbow characteristic/color.

Then a LOL 2000 LiftOff Layer should be placed atop the wafer using a pipette in the same manner. It should be spun at 3000 rpm for thirty seconds, then the substrate should be baked for 10 minutes at 180°C. Finally, SPR 955 CM-0.9 positive photoresist should be dropped on top of the wafer using a pipette, once again attempting to avoid bubbles in the liquid. It should be spun at 3000 rpm for thirty seconds. This is followed by baking the wafer for sixty seconds at 90°C.

2. After the photoresist has been applied and cured, it should be placed into the Heidelberg MLA150 Maskless Aligner. Once the wafer has been aligned with a

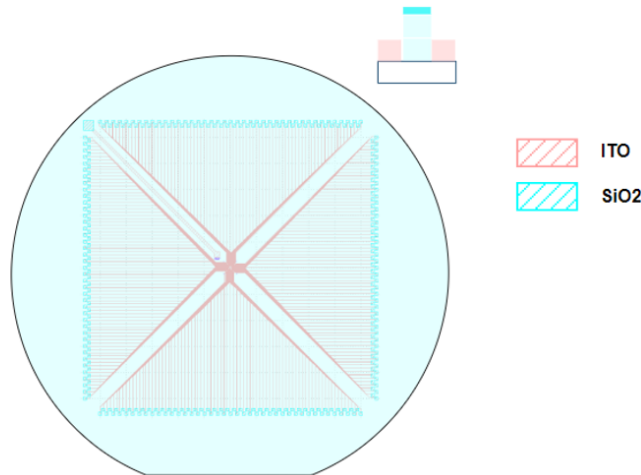


Figure 2.16: After exposure and development, the photoresist (bright blue) covers the entire substrate surface. The only location left exposed is the bond pads. This means that when gold is deposited, the gold will adhere to the ITO on the bond pads but to the photoresist everywhere else.

rotation of 15 mRad or less, the wafer can be exposed with the electrode mask. The mask I designed for this step should NOT be inverted on this tool, as the exposure is directly above the bond pads. Because the photoresist is positive, this will remove the photoresist above the bond pads. The following parameters are used: dose ( $\text{mJ/cm}^2$ ) is 260, defocus is -7, laser is 405 nm, and the power is

100%. After exposure, the wafer is baked at 110°C for sixty seconds. Finally, it is developed in AZ MIF 300 for 120 seconds by vigorously shaking the wafer while holding it submerged with tweezers. The same process is repeated in deionized water for sixty seconds after development to clean it.

3. Using a CHA Industries SEC-600-RAP Multi Wafer Evaporator, gold is deposited on the surface of the substrate. Unfortunately, due to thermal stresses, gold will delaminate if applied directly to silicon dioxide or ITO. To avoid this, a thin layer of titanium is applied first, as gold will bond readily to titanium. Using the system, 0.050 kA of titanium are deposited at 0.2 A/sec. For the titanium layer, set the deposition rate to 0.2 A/sec and deposit 0.050 kA of titanium using Sweep Program 1. For the gold layer, set the deposition rate to 0.2 A/sec for a 1.000 kA deposition, with two ramp periods. Additionally, turn off the sweep program as it is not needed for gold deposition. The first ramp should ramp to 0.5 A/sec of deposition after hitting 0.075 kA, and the second ramp should ramp to 1 A/sec of deposition after hitting 0.350 kA.

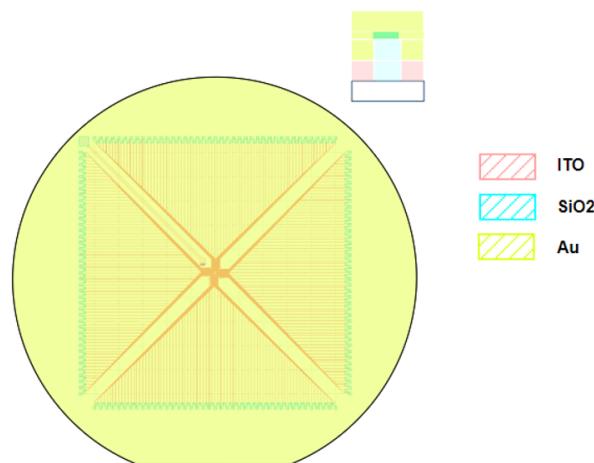


Figure 2.17: After electron-beam PVD, a 100 nm film of gold (shown in yellow) coats the surface of the substrate. However, the gold is only in contact with the ITO on the bond pads. Elsewhere, it is in contact with the photoresist.

4. To perform liftoff, place the wafer into a beaker filled with AZ NMP rinse photoresist remover. Cover the top of the beaker with aluminum foil and place it on an 80°C hotplate. It should be left for 30-45 minutes. Once the gold is visibly peeling and there are flecks of gold in the solution, place the beaker into the heated bath sonicator and sonicate at the lowest intensity to gently remove the remaining photoresist. The intensity may be increased if there are stubborn patches of gold.

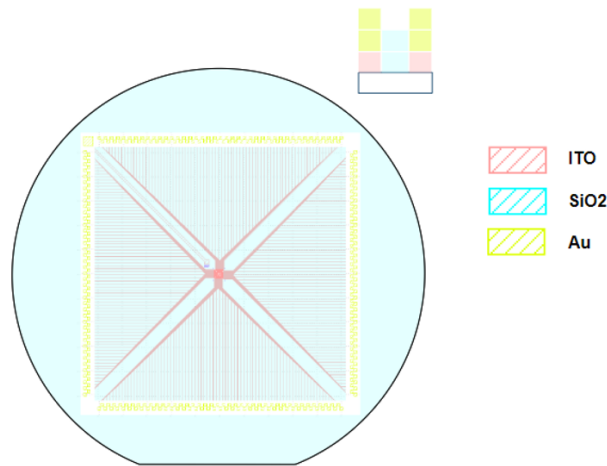


Figure 2.18: Following liftoff, the only gold left on the surface of the wafer is on the bond pads. This electrical contact will ensure that gold to gold wire bonding goes smoothly when assembling the device in section 3.2.

5. To clean the wafer before dicing and remove any debris, the substrate is subjected to a standard sonication clean consisting of 3 minutes of acetone, 3 minutes of isopropyl alcohol, and 3 minutes of deionized water, as before. Then, using the YES ecoclean plasma ash, a 3kW 180°C clean is performed for ten minutes. This strips any residual photoresist from the surface and prepares the surface for new material deposition. After the application of photoresist to protect the surface, the substrate can be diced and is ready to move on to be assembled in the device outlined in section 3.2.

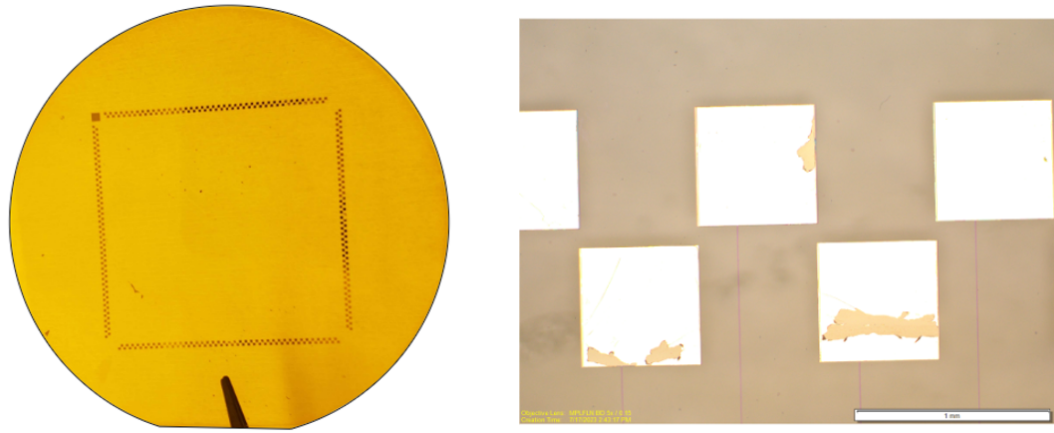


Figure 2.19: On the left is a bird's eye view of the wafer after a successful liftoff process, which has resulted in 100 nm of gold being deposited on the surface of the substrate. Depicted on the right is a close up view of the gold bond pads. Though there is some delamination, enough gold is retained for wire bonding to proceed.

## 2.3 Electrical Resistance

In order to characterize the resistance of the electrodes, a measurement is made by placing a probe at one electrode and another probe at the corresponding bond pad. At a known current at a known potential passing from the probe into the transparent electrode, down the transparent wire, and into the other probe yields the resistance of the material, in accordance with Ohm's Law. Because resistance is proportional to the length of the conductor, electrodes with bond pads towards the center of the substrate (with shorter traces) have lower resistances than the electrodes with bond pads towards the edge of the substrate. By measuring the edge electrode, I characterized the upper bound for the resistance of the 324 electrode devices at  $\sim 50$  kOhms. Similarly, I characterized the upper bound for the resistance of the 64 electrode devices at  $\sim 6$  kOhms.

# Chapter 3

## Electronics Design

Having fabricated the transparent microelectrode array in chapter 2, one might assume that the bulk of the work is completed, and that all that remains is to trivially place this substrate into a magic container where cells proliferate endlessly, and it is easy to stimulate the tissue on the array. Unfortunately, neither of these tasks are trivial. The former is the domain of biologists, and the latter is the domain of electrical engineers—not to mention, the focus of this chapter.

Though many common household appliances (microwaves, dishwashers, ovens, toasters, hairdryers, etc.) may seem simple, the feats of electrical engineering required to build these appliances are quite intricate and complex. It is not an exaggeration to say that the majority of household appliances are more complex than the systems outlined in this chapter. The goals of the electronics designed here is to permit a user to use some external source to apply a voltage to a selection of electrodes in the hopes of stimulating the tissue on the array—science, if you will. Yet, this declaration ought to give the reader a healthy dose of respect for the electrical engineers who provide the backbone of modern day conveniences.

### 3.1 Voltage Stimulation Platform

In order to provide a bridge between a computer and the cells on the MEA, I designed the voltage stimulation platform outlined in the following section. Because cells grown or placed on the array have an unpredictable arrangement with respect to the electrodes, precision experiments which rely on stimulating a series of isolated cells require that voltages be applied to an arbitrary selection of electrodes. To facilitate this, the assembled platform includes four AD5674R multi-channel digital to analog Converters (DACs) which I selected for their low noise specifications, programmable channel selection, and daisy-chain serial peripheral interface (SPI) communication mode. To drive the DACs, I selected a Teensy 4.1 microcontroller for it's 600 MHz clock speed, which is capable of driving SPI communication for all device peripherals.

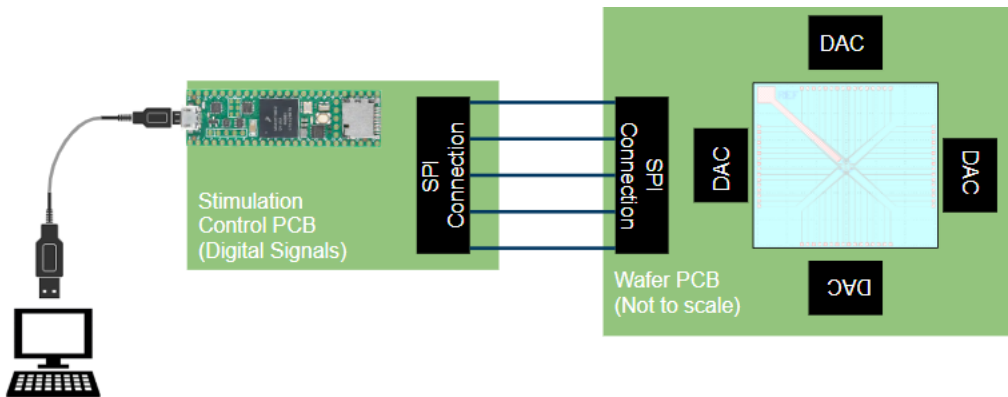


Figure 3.1: The following block diagram represents an outline of the first prototype voltage stimulation platform. A microcontroller (Teensy 4.1) using serial peripheral interface (SPI) communication as a bridge between the AD5674R multi-channel digital to analog converters (DACs) on the printed circuit board (PCB) where the transparent MEA is mounted.

The firmware I wrote in C++ provides a low level framework upon which I built a UI to enable a user to control hyperparameters such as the electrode selection, amplitude, frequency, and duration of applied voltages. I designed the software architecture

to be adaptable to any system using an arbitrary number of AD5674R DACs, allowing future prototypes to seamlessly scale up to higher numbers of electrodes. The prototype presented in this section uses a 64 electrode transparent MEA, fabricated as outlined in section 2.2.1.

### 3.1.1 Electromagnetic Compatibility

When considering electromagnetic compatibility, it is necessary to distinguish between signal ground and functional ground. Signal ground provides a pathway for a signal current to return to its source, whereas functional ground is a ground intended to mitigate issues with electromagnetic compatibility. When designing the printed circuit board (PCB) for the voltage stimulation platform described in section 3.1, my main focus for design constraints was informed by considerations of these types of grounds and generally ensuring electromagnetic compatibility.

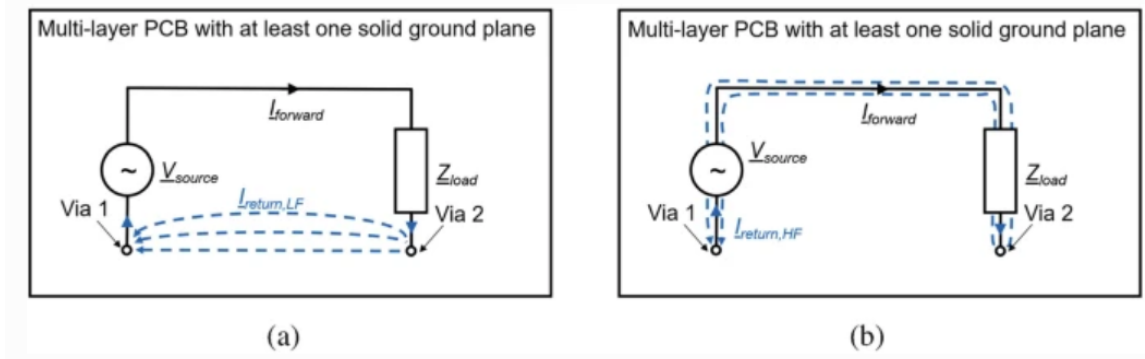


Figure 3.2: In a), the low frequency signal takes the path of least resistance (a straight line) back to the source. In b) the high frequency signal takes a path directly following the signal path back to the source because the inductive reactance of the ground path dominates the impedance. Reproduced from [10]

Because radiated emission due to differential mode current is proportional to the area of the loop formed by current flowing from the source, through the load, and back to the source, is minimized. Diminishing this path length improves signal integrity

and minimizes problems arising from path loss. Because at high frequencies ( $>1$  MHz), the inductive reactance of the ground path dominates the common impedance, the ground return path is likely to follow directly underneath the signal trace. At low frequencies ( $<100$  kHz), the resistance of the ground path dominates the common impedance. Because the lowest resistance between two points in a ground plane is a straight line, the return path of this signal is a straight line [10].

A ground loop is a current loop formed by ground conductors and the ground itself, which can cause issues through interference caused by ground voltage potential difference or magnetic field coupling to the ground loop. In order to prevent ground loops and unintended signal paths from being unintentionally created, all high frequency signal paths are routed without breaks for vias. Additionally to prevent electromagnetic coupling, each of the traces are separated by a distance three times the thickness of the trace.

### 3.1.2 Digital to Analog Conversion

Because it is necessary to control a variety of parameters in the signals applied to the tissue (such as the frequency, amplitude, duration, etc.), these signals are necessarily analog. However, because digital electronics rely on high and low signals to represent zeros and ones, they are robust to path loss and noise. As a result, the majority of modern electronics operate digitally—including the Teensy 4.1 microcontroller driving the voltage stimulation platform. In order to decode these signals and transform them into voltages on the electrodes, a digital to analog converter (DAC) is needed.

Fortunately, the waveforms necessary for the experiments that will be run on this system are biphasic square waves. This simplifies the complexity of the DAC

operations to using software control to output a desired voltage for a desired duration. In general, a DAC has a fixed range of output voltages. The AD5674R DACs selected for the system have a range of 0-5 Volts. Additionally, information is represented by digital “words” consisting of a number of bits, known as the resolution. The DACs in the system represent information relating to the voltage output in 12 bits.



Figure 3.3: By repeatedly sending digital “words” to a digital to analog converter (DAC), a discretized version of an analog signal can be reproduced. On the left is the analog signal, while on the right is the reproduced version of the signal.

Each bit is either a zero or one, permitting  $2^{12}$  (4096) different binary values. These values are mapped to the range of voltages that the DAC can output (ie: in the case of the system DACs, the binary word consisting of all bits set equal to zero represents 0V, whereas the binary word consisting of all bits set equal to one represents 5V) yielding a resolution between steps equal to the range divided by the number of different possible bits. To represent a complex analog signal that varies in time, the DAC rapidly changes it’s output state to match that of the desired signal. For this system, rapidly changing the DAC’s output state is controlled automatically by the software based on the user’s desired signal inputs.

### 3.1.3 Serial Peripheral Interface

The serial peripheral interface (SPI) communications protocol is a modern digital electronics communications bus that ensures synchronous data transfer. One device (in our case, the Teensy 4.1 microcontroller) is designated as the “controller”,

and the other devices (in our case, the four AD5674 DACs) are designated as the “peripherals”. The controller is in charge of orchestrating all communications with the peripherals, and operates the clock.

In a standard SPI setup, each peripheral has four data lines: the clock line, which allows communications across devices to synchronize based on the falling or rising edge of the clock signals; the controller out, peripheral in (COPI) line, which is the line on which the peripheral receives data from the controller; the controller in, peripheral out (CIPO) line, which is the line on which the peripheral sends data out to the controller; and the chip select line, which allows the peripheral to determine if the controller is communicating with it. For this setup, the controller must have the same number of chip select lines as there are peripherals.

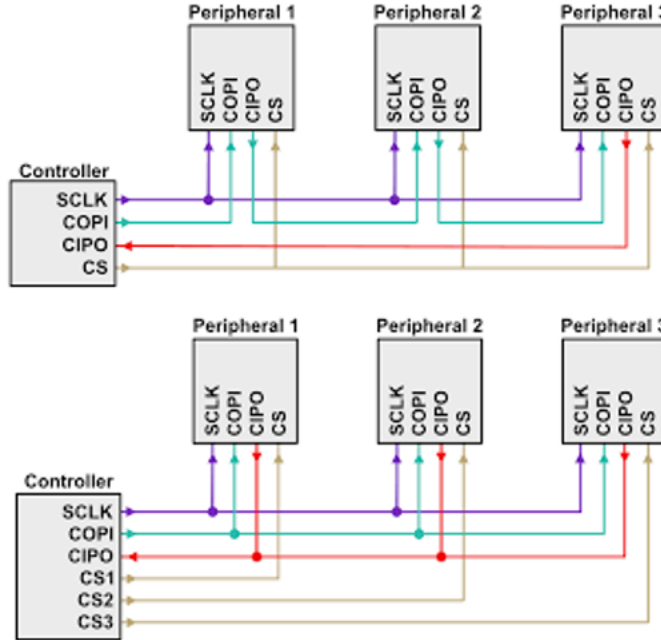


Figure 3.4: The top image demonstrates SPI daisy chain communication, where the input signal ripples across each device and the chip select line enables all devices simultaneously. The bottom image demonstrates standard SPI communication, where each individual peripheral has their own chip select line used to identify which peripheral is being communicated with. Reproduced from [11].

The SPI setup in the voltage stimulation platform instead uses daisy chaining. Rather than have a chip select line to determine which peripheral is being communicated with, the controller sends out a long data stream to communicate with all of the peripherals simultaneously. This works by tying the COPI line of the second peripheral to the CIPO line of the first peripheral so that data ripples out from the first peripheral to the second, and so on and so forth. This requires careful consideration in software design, but ultimately simplifies the electronics by minimizing the number of independent data lines.

### 3.1.4 Software

To control the AD5674R DACs from a computer, I wrote an object oriented architecture in C++ that can be uploaded using arduino software. This means that through a USB connection, any computer with the free-to-download arduino software can run my platform. The code (along with all of my photolithography mask designs and PCB designs) is available on Github [12]. The user interface consists of a list of hyperparameters which a user can edit to determine the resultant stimulation waveform program to be applied to an arbitrary selection of electrodes.

The software includes the following parameters: The frequency in hertz of the waveform, the delay between activating sequential electrodes in the case that multiple electrodes are selected for stimulation (a delay of zero causes simultaneous stimulation), the duration of the positive portion of a biphasic square wave, the duration of a negative portion of a biphasic square wave, the duration during which the signal with the indicated frequency is applied, the duration during which no signal is applied, the number of cycles of signal followed by no signal desired, the amplitude of the positive portion of the biphasic square wave, the amplitude of the negative portion of the

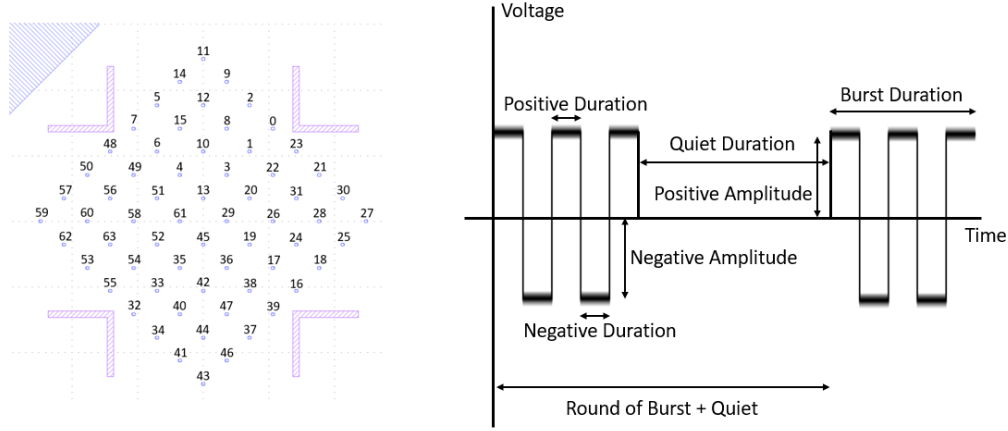


Figure 3.5: To the left is the enumeration of all 64 electrodes in the device. On the right is a plot of the voltage as a function of time for one single electrode, with all independently controllable hyperparameters indicated with arrows.

biphasic square wave, and the list (in order) of the electrodes selected for stimulation.

### 3.1.5 Platform Assembly

Software architecture and design considerations aside, assembling the system is not trivial. I used OSHPark’s PCB fabrication services to order the boards, whose design files are available on my Github [12]. The footprint for the AD5674R DACs contains 28 pins in a 4 mm by 4 mm area. Soldering this by hand is nigh impossible, so the same design files were used to order a 4 mil stainless steel solder stencil using OSHStencil’s services. Aside from the transparent electrodes (whose fabrication is detailed in section 2.2.1), all of the components (capcitors, DACs, voltage regulators, microcontrollers, etc.) can be purchased on Digikey. The final components necessary for assembly are the plastic ring which mounts atop the transparent electrodes to contain the media and the mounting fixture for the inverted microscope. Both of these are 3D printed parts whose design files are also available on my Github [12]. In order to withstand the temperatures associated with sterilizing the array using

autoclaving, the ring was printed using Formlabs Rigid 10K resin which has high thermal resilience.



Figure 3.6: Pictured is the populated VSP system. At the top of platform is the Teensy 4.1 microcontroller, which communicates with a computer via its USB port. The transparent electrodes are accessible through the cutout in the middle, and are attached to the underside of the PCB. The assembly is placed inside the 3D-printed fixture for the inverted microscope. The only assembly component omitted (for visibility) is the ring which contains the media.

For the surface mount components, the process is straightforward. Using the solder stencil, solder paste is applied. The components are placed by hand (using tweezers) onto the pads, and the board is placed inside a reflow oven. The transparent microelectrodes must be attached separately, as the surface tension in the liquefied solder paste causes it to shift. In order to mount the array, I found that it is simplest to use Kapton tape to secure the electrodes to the PCB after depositing solder paste using the stencil. At this point, a heat gun should be used to individually reflow each bond pad to prevent the electrodes from shifting.

After the surface mount components are populated, the through hole female 8 pin connector should be soldered to the PCB. Separately, the male 8 pin connector should be soldered to the Teensy 4.1 microcontroller. This enables the microcontroller to be a separate component that can be removed from one PCB and attached to another, enabling multiple experiments to proceed in parallel with one microcontroller.

## 3.2 BNC Board

Separately, a system was developed to enable an interface between an external function generator and the transparent electrodes fabricated using the recipes outlined in section 2.2.2. The advantage of this system over the voltage stimulation platform outlined above in section 3.1.5 is that it functions with a flexible number of electrodes, whereas the prototype voltage stimulation platform can only function with 64 electrodes. The BNC board system contains arrays fabricated with 324 electrodes, though with further development both systems can scale up to higher electrode density.

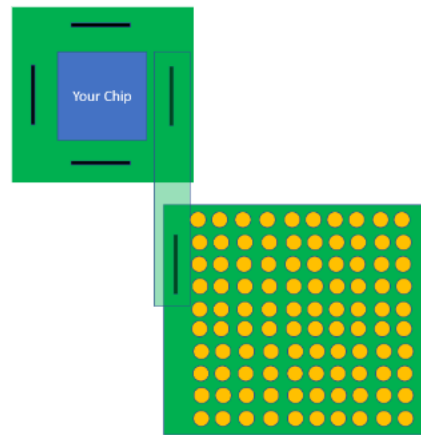


Figure 3.7: The blue square indicates the location of the transparent wafer, mounted on the green PCB. A second PCB acts as a bridge between the PCB with the wafer and the PCB with the BNC connectors.

### 3.2.1 Wire Bonding

To assemble the BNC Board system, the transparent electrodes are adhered to the surface of a PCB using nail polish. Then, to make electrical connections between the PCB and the electrodes on the substrate, the bond pads on the PCB are wire bonded to the bond pads on the substrate using a West Bond ultrasonic wire bonder. Gold to gold wire bonding has a higher success rate than gold to ITO bonding, so it is essential that a layer of gold be deposited on the substrate bond pads.

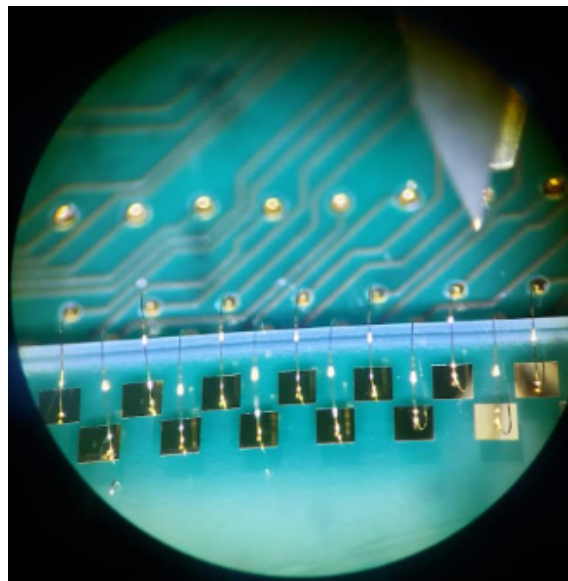


Figure 3.8: Gold wire bonds between the PCB and transparent substrate. The squares are 100 nm thick gold bond pads on the substrate, and the circular pads (partially out of view) are the bond pads on the PCB mount.

# Chapter 4

## Plating Cells

With a transparent microelectrode array assembled and in hand (Chapters 2 & 3), the final step before proceeding to running an experiment is sterilizing the surface of the array and preparing the cells to be plated. Of primary concern is ensuring that the cells survive long enough for experiments to be carried to their conclusion and that the cells adhere to the surface of the microelectrode array. If the cells delaminate, it will not be possible to use voltages to stimulate them. Additionally, the cells need to be in a temperature controlled environment with the appropriate percentage of environmental oxygen available, or else they will die. In general, death is antithetical to the types of experiments the transparent MEA is used for, and its inexorable advance must be slowed.

### 4.1 Environmental Conditions

In our quest to whisk cells away from an untimely demise (in the name of science), a number of environmental conditions are required:

- While cells are plated on the array, they need to be maintained in a temperature

controlled environment held at 37°C degrees

- The chamber holding the MEA must be kept at an environmental composition of 5% CO<sub>2</sub> and 95% O<sub>2</sub>, with 95% relative humidity
- The petri dish (the location on the array enclosed by the ring) should be filled with the media which provides the nutrients for the cells. It is recommended to replace half of this media three times a week. To prepare 100 ml of the media for neurons, the following proportions of ingredients should be prepared:
  - 96.2 mL of Nuerobasal base
  - 1 mL of Glutamine
  - 1 mL of P/S
  - 0.58 mL Sodium Bicarbonate
  - 1.22 mL 45% Glucose

## 4.2 Sterilization

In order to ensure that the cells survive their contact with the microelectrode array, it must be sterilized using the following three step treatment:

1. First, the ring (which will be placed on the array) is sterilized in an autoclave for twenty five minutes at 121°C with water vapor
2. The ring is then glued to the glass service in a class 1000 cleanroom space.
3. Use air plasma for 45 minutes at a bias voltage of 0.15 V

Optionally, the array can be additionally sterilized through exposure to ultraviolet light for a period of half an hour.

## 4.3 Cell Plating

Finally, the following steps should be followed to place the cells on the array. At the end of these steps, the MEA should have cells and be ready to proceed to experiments! Note that in the following steps, the “petri dish” refers to the ring that holds the media above the electrodes. The following procedure is identical to the procedure used by Maxwell Electronics (and indeed, was developed by Maxwell Electronics) [5].

1. Prepare a 1% Terg-a-zyme solution (10 g/L) in deionized water. Always use fresh 1% Terg-a-zyme solution.
2. Add 1 mL of the solution to the surface of the well and keep at room temperature for 2 hours.
3. Remove the solution and rinse out the surface with deionized water. Rinse three times to ensure that no Terg-a-zyme solution remains.
4. Fill the well with 70% ethanol, and let the surface sit for thirty minutes.
5. Once again, remove the solution and rinse out the surface with deionized water.
6. Aspirate the water with a vacuum pump.
7. Fill the petri dish with 1 mL of sterile deionized water
8. Condition the petri dish with 0.6 mL of the cell medium outlined in section 4.1.
9. Cover the petri dish with a lid sterilized using the same procedures outlined in section 4.2. Make sure that the medium does not touch the lid.
10. Place the MEA inside the humidity chamber for two days.

11. Before plating cells, aspirate the cell culture medium and wash once with sterile deionized water. Completely aspirate the surface using a vacuum pump.
12. Prepare 120 mL of 1X Borate buffer by diluting 6 mL of 20X borate buffer in 114 mL of sterile deionized water
13. Prepare an intermediate 7% PEI solution by pouring 1 mL of 50% PEI solution into a 15 mL centrifuge tube and allow it to settle. Add 6 mL of 1X borate buffer (prepared in the previous step) to obtain the intermediate solution
14. Prepare a final 0.07% PEI solution by diluting 1 mL of intermediate 7% PEI solution in 99 mL of 1X Borate buffer.
15. For sterilization before use, pour through a 0.22 micron filtration unit.
16. Add 50  $\mu$ L of the final PEI solution to directly cover the electrodes.
17. Cover the petri dish with an autoclaved, sterile lid, and incubate in the humidity chamber for 1 hour.
18. Aspirate the solution completely using a vacuum pump.
19. Wash three times with 1 mL of sterile deionized water.
20. Aspirate the surface completely using a vacuum pump. Let the surface dry for an hour.
21. Dilute Laminin in the cell culture medium, then add 50  $\mu$ L to the center of the electrode surface.
22. Cover the petri dish with an autoclaved lid, and allow it to incubate in the humidity chamber for an hour.

23. Aspirate the surface completely using a vacuum pump.
24. Plate cells by adding cell suspension to the electrodes. Then cover and incubate for an hour.
25. Finally, carefully fill with 0.6 mL of culture medium so as to avoid delaminating the cells.



Figure 4.1: Cardiomyocyte-based heart organoid plated on a 324 electrode transparent MEA, as outlined in section 3.2. Though it is not aligned with the electrodes (and thus is not a good candidate for experiments), it does display adherence of the cells to the array alongside a visualization of the transparent electrodes.

# Chapter 5

## Results

Throughout this work, I have motivated the development of a transparent MEA for the combination of voltage stimulation and optical imaging techniques. Having outlined the manner in which the transparent electrodes are fabricated, the considerations behind certain design choices, the electronics which serve as a bridge between the electrodes and a human interface, and the principles by which the system works, I present the result that I have succeeded in developing a proof-of-concept prototype transparent MEA.

Ideally, this prototype should abstract all of the principles of its operation—the electrical engineering, nanofabrication, and the computer engineering—so that someone with no practical knowledge in these areas retains the flexibility to design and execute any arbitrary experiment that they would like to. Indeed, my aim throughout development was to enable this exact scenario, as an instrument is only useful insofar as much as it can be used. It follows that the only thing that remains is to outline how to operate the system.

## 5.1 System Operation

As mentioned above, all of the principles of operation of the system are abstracted to the interface between the electrodes and the human operating the MEA. Primarily, I am referring to the system developed in Section 3.1, as the system interface developed in Section 3.2 requires manually plugging and unplugging cables into a board with 81 BNC ports, or stimulating large swathes of electrodes simultaneously with no selectivity.

In any case, this interface consists of the Teensy 4.1 Microcontroller, a USB cable, and the operator’s personal computer. The Teensy 4.1 is compatible with Arduino’s IDE (with the Teensyduino add-on), so all of the code I developed for this project is written in C++, hosted on my personal Github [12], and tested/debugged for Arduino’s IDE. Prior to running the system, the following steps should be followed, in the following order:

1. Download the Arduino 2.0x IDE from Arduino’s website. It is available for free. It is worth noting that I have an older version of the Arduino IDE and successfully ran the software and the following steps with Arduino 1.8.16
2. After downloading the IDE, open it. Because this development environment is used for a number of different microcontrollers, Teensy 4.1 has an additional installation to allow the IDE to drive the Teensy. Click on “File” in the upper left hand side of the IDE, then “preferences.” On Mac OS, click “Arduino IDE,” followed by “Settings.” In “Additional boards manager URLs”, copy and paste the following text: [https://www.pjrc.com/teensy/package\\_teensy\\_index.json](https://www.pjrc.com/teensy/package_teensy_index.json)
3. In the Arduino 2.0x IDE, the board manager can be accessed from the sidebar. In the Arduino 1.8.16 IDE, it is accessed via “Tools” on the bar at the top,

selecting “Board: [The Last Board You Used]”, and finally selecting the Board Manager. There, you can search for Teensy and click install. When I ran the system, I installed Teensy 1.58.1, though it is possible that this version is incompatible with the Arduino 2.0x IDE. Future users should be sure to install a version of the software compatible with their IDE.

4. Now that the IDE is ready, note that there is an additional piece of software that is required for the system to function. The files that I programmed (which contain the instructions for a given experiment!) are in C++, which needs to be compiled and converted into machine code so that the microprocessor can understand it. Then, these files need to be loaded onto the microprocessor. The Teensy 4.1 uses a different loader than the standard loader used for loading these machine code files onto standard Arduino boards. To download this loader and other necessary support files, users will need to run the Teensyduino Graphical Installer. This should happen by default on the previous step if running in the Arduino 2.0x IDE. If it does not, you will need to install these files on your own. They can be accessed on the Teensy 4.1 website at the following url: “<https://www.pjrc.com/teensy/loader.html>”
5. To test that all of the associated software is correctly set up on your computer, plug the USB cable into the microcontroller. You should see the orange LED light up and begin to blink as soon as the Teensy is connected. Open the “Blink” sketch, which is an example sketch that is provided. Change the frequency or duration of the blinks in the provided example, then attempt to upload this sketch to the Teensy. You may need to press the button on the Teensy to cause the loader to work for the first upload. If successful, excellent! You’re ready to run any arbitrary experiment that you would like to on the system. Otherwise,

useful tips for troubleshooting can be found on the Teensy 4.1 website.

6. To download the software itself, go to my Github [12]. Open the directory titled “64 Electrode Stimulation.” Inside this directory are a number of other directories and files related to this project. The code for driving the system is contained in the directory titled, “Stimulation Board.” Downloading all of the files in this directory and opening them in the IDE will allow the system to be run.
7. Admittedly, the UI leaves much to be desired, as it requires a user to directly edit hyperparameters in the file titled “Stimulation\_board.ino” instead of having a nice, pretty graphical user interface. In my defense, it was a non-critical component of the system, so it got pushed to the bottom of my to-do list and ultimately did not get implemented. Instructions for the definition and unit of each hyperparameter are located in the file itself and outlined in Section 3.1.5.  
Happy experimenting!

# **Chapter 6**

## **Conclusion**

Finally, having presented the construction and operation of the transparent MEA, all that remains is to discuss possible and proposed experiments that can be run with the system as is. Of course, since the system is only a proof-of-concept prototype, it is also worth delving into how future improvements should be implemented, pitfalls, and areas that should be improved in the next iteration or generation of these devices.

### **6.1 Experiments**

Because this prototype only includes electronics for stimulating the cells on the transparent array, it is suitable for a subset of experiments in which cells are to be stimulated and data is collected by observing through the transparent electrodes. As always, the subset of organoids and cells which can be experimented on are those which are electrically active, which primarily includes cardiomyocytes for the heart and neurons for the brain.

Here I'd like to mention the experiments proposed by our collaborators for each

of these types of cells, starting with cardiomyocytes. A group of cardiomyocytes which together collectively comprise a heart organoid will beat in time with each other, at a frequency observable by viewing the organoid with a camera recording at a sufficiently high rate. An experiment proposed (and at the time of writing, currently in the process of being carried out) is to attempt to induce changes in the frequency that an organoid heart is beating through stimulation through all electrodes simultaneously at an alternate frequency.

A similar experiment with neuronal cultures has been proposed by our collaborators to induce action potentials in neurons to demonstrate the viability of the system. After establishing the efficacy of the system, it is proposed that neurons atop the array be identified visually for contact with electrodes. After doing so, four neurons in contact with electrodes should be selected for delayed stimulation using the electrode selectivity feature. By stimulating these neurons with biphasic square waves in sequence, it is hypothesized that when stimulation ceases, these neurons will continue to fire in the same pattern. Ostensibly, this would provide evidence for the classic adage that “neurons that fire together, wire together.”

## 6.2 Next Steps

The system I developed is not without its limitations. First and foremost, it lacks the ability to read out extracellular voltage signals from the cells on the array. This significantly limits the breadth and depth of experiments that can be carried out with the system. Fortunately, I developed the current prototype with the idea in mind that a method of reading out voltage signals would soon follow.

For this, I recommend implementing an RHD2164 Intan Digital Electrophysiology chip into the current PCB. This component possesses the capability to amplify, filter,

and read out signals using a custom SPI protocol, and was specifically designed for neurobiology applications. To simplify much of the electronics design process, I recommend purchasing an Intan RHD recording system, which allows a user to simply plug the recording system directly into the PCB rather than attempting to integrate the custom SPI protocol into the software on the Teensy. However, if electing to go the DIY approach, I would like to note that the Intan Electronics website contains designs for the FPGA implementation for precisely this SPI protocol. Additional design considerations should include whether or not an additional amplification stage for signals (prior to implementation of the Intan RHD2164) is required.

Another limitation of the system is the fact that it only possesses 64 electrodes in a 2 mm by 2 mm area, whereas commercial arrays have significantly higher electrode densities over larger areas. Of course, scaling up to higher electrode densities imposes significant design constraints and complexity, but I have done the best that I can to create a modular system for the stimulation stage which is capable of easily scaling to integer multiples of 64. A reasonable second prototype should be able to reach 256 electrodes in the without needing to change the wafer foot print (3 cm x 3 cm).

Scaling up the system to include additional electrodes will require designing a new wafer with the desired number of electrodes in KLayout and Altium. When undertaking this process, I highly recommend optimizing the design to reduce the resistance of traces. In general, the resistance is proportional to the length of traces and inversely proportional to the width of traces. Thus, any possible efforts to reduce the length and increase the width of traces should be undertaken, as high resistance will cause additional complications in amplifying, reading out, and sending in signals. As this may pose a significant bottleneck, it may be worth considering alternate transparent materials from which to fabricate the transparent MEA, such as PEDOT:PSS.

Finally, to address the issues caused by resistance in PCB and wafer traces is an output amplification stage after each of the digital to analog converters to ensure that there is limited signal attrition. As noted in Section 2.3, the electrodes themselves have resistances ranging from  $2\text{ k}\Omega$  to  $6\text{ k}\Omega$ . The DACs have a built-in output amplification stage, but it saturates at  $1\text{ k}\Omega$ . This implies that any output voltage stipulated by a user is reduced to a signal strength of a half to a sixth of the original signal amplitude.

Fortunately, the DAC has an output voltage permitting a biphasic square wave with a maximum amplitude of 2.5 Volts. Since the range of stimulation voltages required for the majority of experiments as posited by the literature is 50 millivolts to 200 millivolts. To be able to drive a waveform which permits access to the upper range of 200 mV, the maximum resistance on a given electrode must be limited to  $12.5\text{ k}\Omega$ , as this would reduce a 2.5 Volt signal to 8% of its initial strength, or 200 millivolts. Thus, some combination of reducing resistance and providing an output amplification stage for the DACs is necessary for future prototypes. To any future developers, I wish you the best of luck!

# Bibliography

- [1] J. Barbuzano, “Organoids: A new window into disease, development and discovery.”, <https://hsci.harvard.edu/organoids> 2017.
- [2] Z. Z., C. X. and D. A. et al., *Organoids*, *Nature Reviews Methods Primers* **2** (2022) 94.
- [3] G. Buzsáki, C. Anastassiou and C. Koch, *The origin of extracellular fields and currents — eeg, ecog, lfp and spikes*, *Nature Reviews Neuroscience* **13** (2012) 407.
- [4] M. Lin and M. Schnitzer, *Genetically encoded indicators of neuronal activity*, *Nature Neuroscience* **19** (2016) 1142.
- [5] B. M., M. J. and L. P. et al., *A 1024-channel cmos microelectrode array with 26,400 electrodes for recording and stimulation of electrogenic cells in vitro*, *IEEE J Solid-State Circuits* **49** (2014) 2705–2719.
- [6] J. X. Zhang and K. Hoshino, *Molecular Sensors and Nanodevices*. Elsevier, 2019.
- [7] H. Instruments, “Maskless laser lithography.”, <https://heidelberg-instruments.com/core-technologies/maskless-laser-lithography/> 2023.
- [8] Corial, “Reactive ion etching (rie).” ,  
<https://corial.plasmatherm.com/en/technologies/reactive-ion-etching-rie> 2023.
- [9] Intan Technologies, *Digital Electrophysiology Interface Chip*, 9, 2013.
- [10] R. B. Keller, *Design for Electromagnetic Compatibility—In a Nutshell*. Springer, 2022.
- [11] S. Electronics, “What is the spi communication protocol.” ,  
<https://soldered.com/learn/what-is-the-spi-communication-protocol/> 2023.
- [12] S. Herman, “Transparent-me.” ,  
<https://github.com/Jezen5Volk/Transparent-MEA> 2023.